The Nucleus **56**, No. 3 (2019) 112-122

www.thenucleuspak.org.pk

The Nucleus
ISSN 0029-5698 (Print)
ISSN 2306-6539 (Online)

Simulation Modeling of Multi-Junction Solar Cell for Efficiency Improvement

M.A. Adnan Ali* and S. Akram[1]

Electrical Engineering Department, Institute of Southern Punjab, Multan, Pakistan

[1]Chemistry Department, Government College University, Faisalabad, Pakistan

ARTICLE INFO

Article history:
Received: 04 July, 2018
Accepted: 21 February, 2020
Published: 03 March, 2020

Keywords:
Solar Cell
Modeling
Multi-junction Solar Cell
Simulation
Triple-junction Solar Cell

ABSTRACT

Current trends in the design of Multi-Junction Solar Cells (MJSC) and quantum dot applications form the backbone of the Concentrated Solar Photovoltaic (CSPs) Systems. There are a number of developments in solar power technology because of their improved power production, high efficiency, high absorption coefficients and cost-effectiveness. Selection of solar photovoltaic (PV) materials of different band gap energies to absorb complete solar spectrum is close to a reality with decrease in price to performance ratio. This paper presents a generalized MJSC simulation model. The present model assumes a mathematical approach, investigating solar cell characteristic curves including current density (J_{sc}) and power (P) curves concerning the applied voltage for a different number of junctions and by varying the material properties of the multi-junction (MJ). The proposed model simulates different parameters and performance characteristics of two different natures of MJSC including InGaN/AlGaAs/InGaAs Triple Junction Solar Cell (TJSC) and InGaN/InGaN/AlInP/AlInP/AlGaAs/AlGaAs/AlGaAs Seven-Junction Solar Cell. Simulation results presented in this paper are in agreement with experimental results. Solar cell parameters including short circuit current (J_{sc}), open circuit voltage (V_{oc}), leakage current (J_o), output power (P_{out}) have also been calculated in this work. The efficiency (%η) of a TJSC for visible light, ultraviolet (UV), visible and infrared (IR) light is presented. The efficiency (%η) of seven junction solar cell is calculated to be 63%. Characteristic curves of the solar cell are plotted as a function of voltage for different concentration levels and the number of junctions, which helps to design a solar power array that can operate to its peak power point. The objective of this research is to improve the overall efficiency of MJSC.

1. Introduction

The fossil fuels are used as energy source for different purposes. The significant drawbacks of fossil fuel as an energy source are limited availability for next 50-100 years and emission of greenhouse gases (i.e. CO_x, NO_x, SO_x, H_gO_x). Renewable energy resources, i.e. wind and solar power can be used as an alternative to fulfil the requirement of energy demand [1].

Solar power is clean, environment-friendly, free with abundantly available. Earth receives a small portion of the energy from the sun which is equal to 1.74 x 10^{11} MW. On average, solar radiations of 84 minutes only can fulfill total energy demand on earth for the whole year [2].

1.1 Single-Junction Solar Cell (SJSC)

The solar radiation is composed of different wavelengths of light out of which some amount of light is absorbed by single-junction solar cell and converted into electrical energy [3]. The efficiency of single-junction solar cell is low and most of the photons penetrate and are dissipated into heat [4].

1.2 Multi-Junction Solar Cell (MJSC)

Recent research into PV systems has led to the invention of advanced solar cells called MJSCs, which use broad range spectrum of light for better performance and efficiency. MJSC use multiple combinations of PV junctions, or bandgaps, which are stacked on one another with intrinsic materials or tunnel junctions. These solar cells are combined in such a way as to absorb a defined region of the solar spectrum to create a MJSC with efficiencies higher than 45%. Different combinations of PV solar cells have different physical properties [5–8]. Studies show that substantially higher efficiencies of solar cell can be achieved by increasing the multiple PN junctions of different materials or layers [5]. In MJSCs, multiple III-IV materials are stacked in descending order, i.e. materials with higher bandgap energies are placed on top, while material with lower bandgap energy is placed at the bottom of the cell. Similarly, multiple PN junction cells are stacked on each other to form a single MJSC. More energy can be captured in this way, as each PN junction will yield current in response to different solar spectrum. Overall efficiency of MJSC is high as compared to traditional solar cells as more photons can be captured and converted into electricity [9–11].

1.3 The Efficiency of Solar Cell

The ratio of power generated in the solar cell to irradiance received by the solar cell is called efficiency (η). The maximum theoretical efficiency of traditional SJSC is 33.16% at standard test conditions (STC) [12, 13]. The efficiency of SJSC is relatively low, as most of the penetrated photons are dissipated into heat [5]. This is primarily due to extensive distribution of photons. This limiting efficiency (η), is known as the Shockley-Queisser limit, and is determined from the fact that open circuit voltage (V_{oc}) is limited by the bandgap energy of the material. Photons with energies higher than bandgap are absorbed and photons with energies below the bandgap are not absorbed and are lost as heat.

*Corresponding author: adzee17@hotmail.com

The efficiencies of solar cells are steadily increasing and have ranges 20-25% for Single Junction (SJ), 22%-30.3% for Dual Junction (DJ), 30-40 % for Triple Junction (TJ) and 37-46% for Quadruple Junction (QJ) [14-19]. Theoretical limiting efficiency for an infinite number of PN junctions is about 86.8% under highly concentrated sunlight at air mass AM° and temperature 25°C [20, 21]. However, the cost of MJSC is 15- 20 times higher as compared with the cost of SJ solar cell due to the complicated manufacturing process. Presently, MJSCs are capable of generating approximately double power as compared to the power generated by traditional solar cells [8]. Table 1 shows the SJSC efficiency for different materials [22].

Table 1: SJSC Efficiency [22].

Type of Solar Cell	Efficiency (%)
Silicon (Monocrystalline)	26
Silicon (Multi-crystalline)	20.7
Silicon (Thin transfer film)	21.3
GaAs (Gallium Arsenide) thin film	28.5
GaAs (Multi-crystalline)	18.7
InP (Indium Phosphide) Monocrystalline	22.3
CIGS (Copper Indium Gallium Selenide)	20.3
CdTe (Cadmium Telluride)	21.3
Silicon (Amorphous)	10.3
Silicon (Microcrystalline)	11.5
Dye-sensitized	12.1
Organic thin-film	11.1
Organic (Mini module)	9.7

2. Structure of MJSC

2.1 Physical and Mathematical Model of a Solar Cell

The generalized physical structure model of a MJSC may be formed by arrangement of solar cells in series. A generalized mathematical model of P-V cell has been discussed in literature [23–26]. The basic equivalent model of the solar cell consists of photocurrent sources, a diode, a series resistors describing an internal resistance to the current flow and shunt resistor expressing a leakage current. The performance of P-V array system depends on its output parameters (voltage, current and power) of P-V array vary as functions of solar irradiation level, temperature (T) and load current.

The I-V and P-V characteristics curves are given by the following equations:

$$\mathrm{J} = J_{sc} - J_0[\exp\left(\frac{q(V+JR_S)}{AkN_sT}\right) - 1] - \frac{V+JR_S}{R_{sh}} \tag{1}$$

The leakage current is expressed as:

$$J_0 = \frac{G}{1000}(J_{sc} + \mu_{sc}(T - 298)) \tag{2}$$

$$\mathrm{J} = J_{rs}[\frac{T}{T_n}]^3 \exp[\frac{qE_g}{kT}\left(\frac{T}{T_n} - 1\right)] \tag{3}$$

The output power is given by:

$$P_{out} = V_{oc}(\mathrm{t})J_{sc}(\min) \tag{4}$$

$$\mathrm{F.F} = \frac{P_{max}}{V_{oc}J_{sc}} \tag{5}$$

Where

J = Current density (A/cm^2)

G = Irradiance (W/m^2)

μ_{sc} = Coefficient of temperature for short circuit current (A/K)

J_0 = Saturation current or leakage current of the diode (A)

J_{sh}= Leakage current in parallel resistor

J_{ph} = Photon current

V = Voltage imposed on the diode (V)

A = Ideality factor based on PV Cell Technology

Ns = Number of cells connected in series and

V_T = Thermal voltage

T = Actual cell temperature (K)

k = Boltzmann constant (1.381 x 10^{-23} J/K)

q = Electron charge (1.602 x 10^{-19}C)

R_s = Series resistance (Ω)

R_{sh} = Parallel resistance (Ω)

T_n = Cell temperature at STC

ΔT = T-T_n (Kelvin)

E_g = Bandgap energy

J_{rs} = Reverse saturation current

V_{oc} = Open circuit voltage (V)

N_P = Number of PV modules connected in parallel

A variable load resistance (R) can be connected to the solar cell to study the behavior at changing loads.

When, R (open circuit) = ∞ $\quad$ $\mathrm{V} = V_{oc}\mathrm{J} = 0$

When, R (short circuit) = 0 $\quad$ $\mathrm{V} = 0 \quad \mathrm{J} = J_{sc}$

From above, we can find that R should be adjusted in such a way that maximum power (P_{max}) is dissipated at the load end. At this adjusted load, P=P_{max}, J=J_{max}, and V=V_{max}.

The equivalent circuit and Simulink model of P-V cell is shown in Fig. 1.

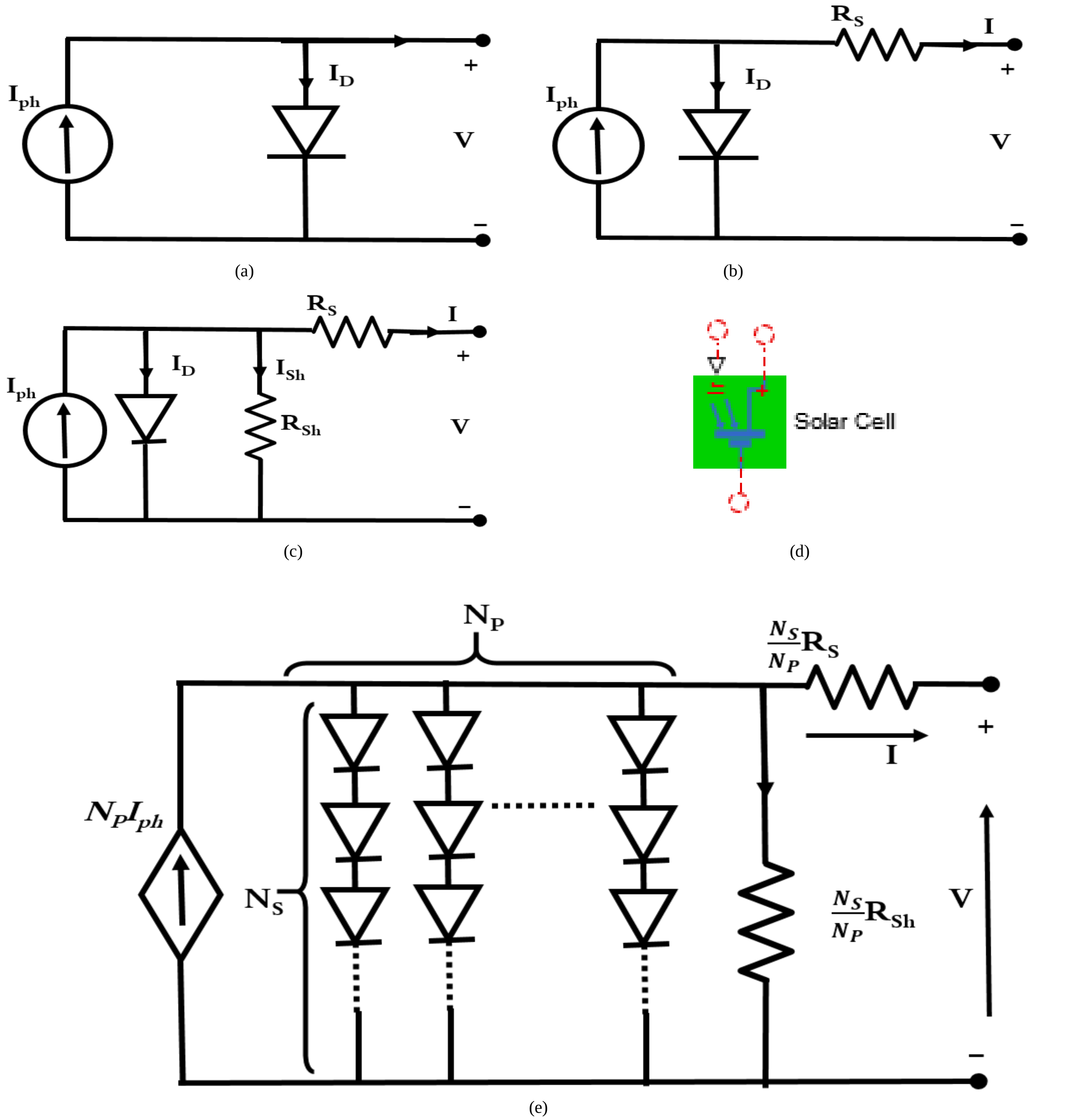

Fig. 1: Simulink model and equivalent circuit of a solar cell (a) Ideal single diode model, (b) Practical model with Rs, (c) Practical model with Rs and Rsh, (d) Simulink model and (e) Equivalent circuit of a solar array.

2.2 Multi-Junction Model

The MJSC model is the combined representation of all PV junctions with short circuit current as its series matched current, series and parallel resistances, whereas the open circuit voltage is the sum of the junction voltages. Tunneling in a MJSC is the process of fast driving charge carriers across the potential barrier. The tunnel diode causes an undesirable situation when it is modeled in series with a MJSC model. This is because of a highly non-linear relationship between current density and applied voltage. The equivalent circuit of a solar array is shown in Fig. 1.

3. Calculation of Performance Parameters for III-V MJSC

Bandgap energy (E_g) and Lattice Constant (LC) are the two essential parameters in design considerations of MJSC. LC refers to the spacing between the molecules of a crystal structure and must match for all of the layers. Different bandgap energies can be obtained from different composition of PV materials. Bandgap energies are selected in such a way that each layer receives equal power and generates equal current. TJSC with bandgap energies 1.8/1.4/0.67 eV has an efficiency of around 30%. The efficiency of TJSC cell can be increased by adjusting bandgap energies. After adjustment of bandgap energies (2.0/1.2/0.67 eV), efficiency is about 40% due to the equal current generated in each sub-cell. Fig. 2 shows the combination of bandgap energies and LC for different compositions (X) of $In_{1-X}Ga_XAs$ as the bandgap energy and LC depends on material composition (X).

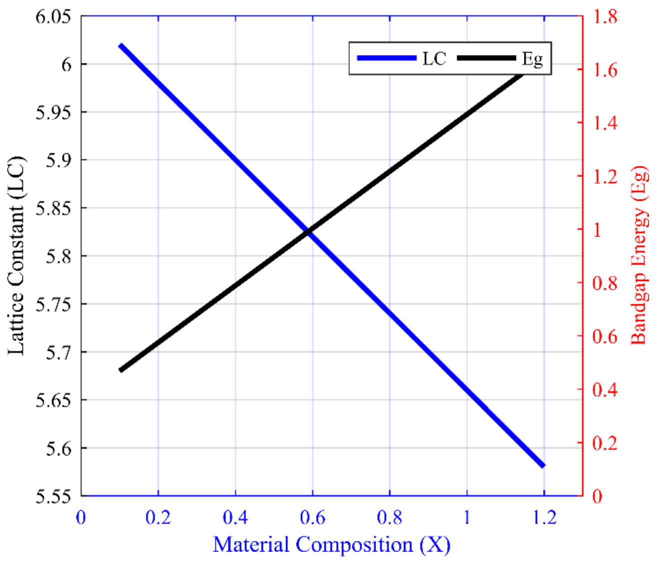

Fig. 2: E_g and LC for different compositions (X) of $In_{1-X}Ga_XAs$.

Bandgap energy can be achieved easily by different combinations of PV materials; however, LC matching is difficult. If lattice mismatched, cell materials are made of different III-V alloys, the molecular structure deforms and causes resistance in the flow of J_{sc}. To avoid deformation of crystal structure in MJSC, all PV material compounds are grown on each other to be lattice matched to the same substrate [27, 28].

LCs and bandgap energies (E_g) of different material combinations can be calculated as:

$$LC(Ga_{1-X}In_XP) = LC_{(GaP)}X + LC_{(InP)}(1-X) \quad (6)$$

$$E_g(Ga_{1-X}In_XP) = E_{g_{(GaP)}}X + E_{g_{(InP)}}(1-X) \quad (7)$$

Where

X = Material composition (0.00-1.00)

Bandgap energy (E_g) and temperature (T) of semi-conductor materials are inversely proportional to each other.

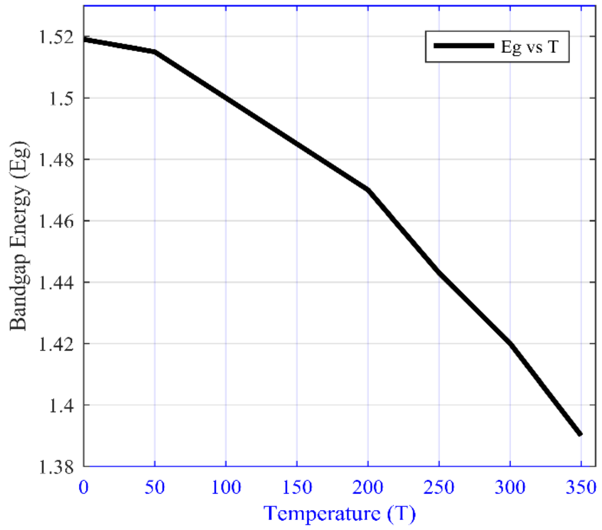

Fig. 3: Effect of temperature (T) on bandgap energy (E_g).

Fig. 3 shows the effect of temperature on bandgap energies. Equations obtained from [29-31] can be used to calculate the relationship between bandgap energies and temperature.

$$E_g(T) = E_g(0) - \frac{\alpha T^2}{T+\beta} \quad (8)$$

Where

α = Temperature coefficient (meV/K)

β = Constant

For GaAs

α= 0.5405 meV/K

β=204 K

Short circuit current for given spectral irradiance and current density can be calculated using Plank's law. Power density is 62.7 MW/m^2 at the surface of the sun. The power density at the surface of the earth is given by:

$$P_E = P_S X \frac{R}{d} \quad (9)$$

Where

P_E = Power density at the surface of earth

P_S = Power density at surface of sun (62.7 MW/m^2)

R = Radius of sun (7.5 x 10^8 m)

d = Distance between sun and earth (1.5 x 10^{11} m)

Power density calculated at earth's atmosphere is reduced to 1367 Watt/m^2.

Spectral irradiance as a function of wavelength and temperature (Planck's law) is given by:

$$bd\lambda = \frac{2\pi hc^2}{\lambda^2} \frac{1}{e^{\frac{hc}{\lambda kT}}-1} \quad (10)$$

Where

b = Spectral irradiance

v = Frequency

h = Plank's constant ($6.626e^{-34}$)

c = Speed of light ($3e^{8}$ m/sec)

k = Boltzmann constant ($1.38066e^{-23}$ J/K)

λ = Wavelength

T = Temperature of sun in K

$$bd\lambda = 2.15x10^{-5}x10^{-9}\frac{2\pi hc^2}{\lambda^5}\frac{1}{e^{\frac{hc}{\lambda kT}}-1} \quad (11)$$

The spectral response (SR) calculates current generated by each watt power of incident light for a specified wavelength. Where, External Quantum Efficiency (EQE) is the ratio of number of generated electrons to number of incident photons [32, 33]. Relationship of spectral power with wavelength (λ) on surface of earth and sun is shown in Figs. 4 and 5, respectively. Relationship of spectral power and current with wavelength (λ) is shown in Fig. 6.

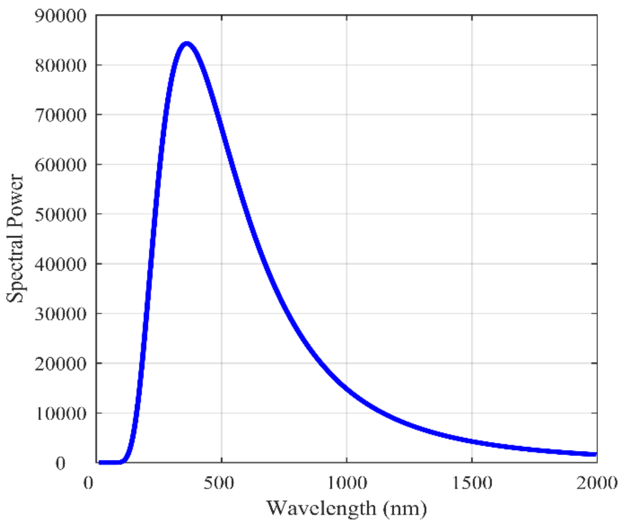

Fig. 4: Spectral power (Surface of the sun).

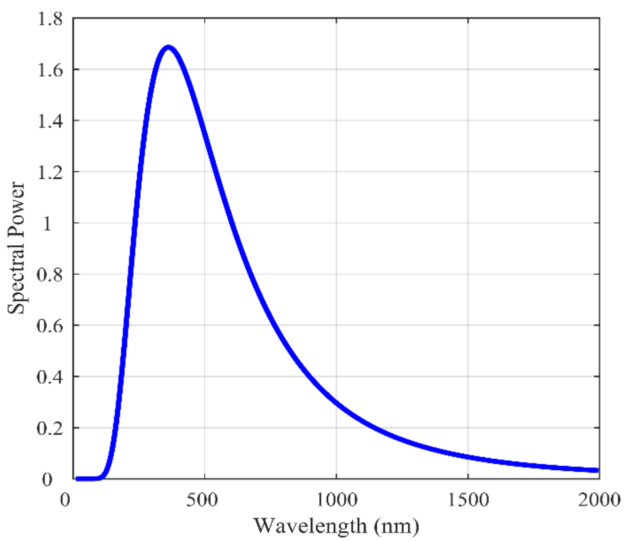

Fig. 5: Spectral power (Earth's atmosphere).

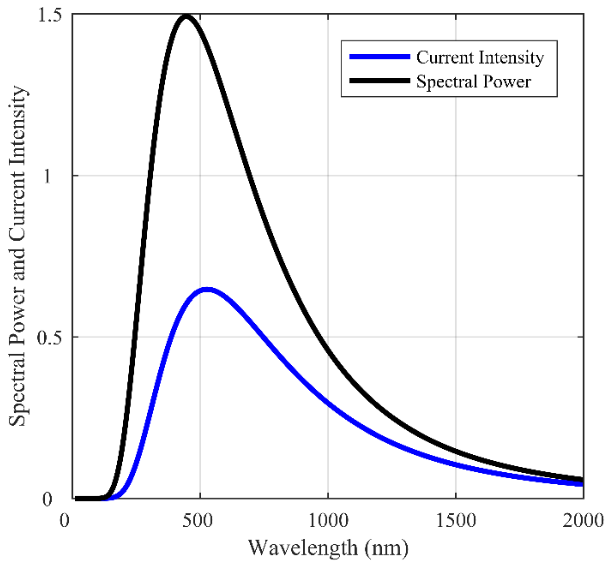

Fig. 6: Spectral power and current intensity vs wavelength (λ).

$$SR(\lambda) = \frac{q\lambda}{hc}EQE \quad (12)$$

In a MJSC, all the PV cells are coupled in series. If EQE is 100% or all incident photons generate electrons, then the total short circuit current can be calculated as [19]:

$$J_{sc} = \int_{\lambda 0}^{\propto} SR(\lambda).E_{B\lambda}d\lambda \quad (13)$$

The Leakage current is given as:

$$J_o = A.e^{(-\frac{qE_g}{k.T})} \quad (14)$$

Where, A denotes the ideality factor [21].

The Open Circuit voltages V_{oc} for each cell can be calculated as:

$$V_{oc}(x) = \left(\frac{kT}{q}\right)\log\left(\frac{J_{sc}(x)}{J_o(x)} + 1\right) \quad (15)$$

The subscript x denotes the number of PV cells used, i.e. (1, 2,3…n). Total voltage is given as:

$$V_{oc}(total) = V_{oc}(1) + V_{oc}(2) + \cdots \ldots \ldots + V_{oc}(n) \quad (16)$$

4. Simulation Model of MJSC

The presented MATLAB/Simulink model is used to simulate and investigate the performance characteristics and cell parameters of the MJSC, i.e. Open Circuit Voltage (V_{oc}), Short Circuit Current (J_{sc}) and power. To achieve maximum efficiency for same LC (angstroms or nm), Bandgap Energy (E_g) can be adjusted using different PV material compositions. LC refers that the spacing of the molecules in a crystal structure must be matched for all the layers. In MJSC, III-V PV materials of different compositions are grown directly on top of other layers with the same substrate. The molecular structure of MJSC layers will be deformed if LC is different for two or more subcells which cause the decrease in cell current. In a MJSC, the current and power distribution should be the same in each cell to enhance efficiency [27, 33, 34].

In this simulation, visible spectrum of light (400-700 nm) is used to calculate efficiency and other parameters of SJSC, TJSC and seven junctions solar cell. UV, visible and IR light spectrum (100-1000 nm) is used to calculate the performance parameters of TJSC. In this work TJSC $Ga_{0.5}In_{0.5}P$/ $Ga_{0.95}In_{0.05}As$/Ge having bandgap energies of 1.8/1.4/0.67 eV respectively and same LC (5.66 A) is presented. The calculated efficiency of this MJSC is 31.5% for 100% EQE. Efficiency can be increased up to 45% if power and current distribution in each cell become the same. The efficiency of TJSC (InGaN/AlGaAs/InGaAs) is found to be low (22%) as power density, and current density of the UV light spectrum is low and causes decrease in efficiency.

In the simulation, efficiency is calculated for different temperatures and suns (1 sun means 1000 W/m^2). The efficiency of MJSC slightly increases as numbers of suns increases and decreases as the temperature decreases. Efficiency and other cell parameters can be calculated at different atmospheric condition.

4.1 TJSC for UV, Visible and IR Light Spectrum

In this simulation, UV, Visible and IR light spectrum is used to calculate efficiency and other parameters of TJSC ($In_{0.11}Ga_{0.89}N/Al_{0.47}Ga_{0.53}As/In_{0.23}Ga_{0.77}As$). The calculated efficiency for TJSC is 21.9% for UV (100-400 nm), Visible (400-700 nm) and IR (700-1000 nm) range.

Changing the materials composition (X) to match the LC and wide bandgap energy for the TJSC is mentioned in Fig. 7. Cumulative short circuit current and minimum short circuit current calculations are shown in Fig. 8.

4.2 TJSC and Seven Junction Solar Cell for Visible Light Spectrum

Materials used for TJSC are $In_{0.24}Ga_{0.76}N$/ $Al_{0.82}In_{0.18}P$/ $Al_{0.65}Ga_{0.35}As$ having bandgap energies (2.75/2.25/1.9 eV) respectively. In this simulation, visible spectrum of light (400-700 nm) is used to calculate efficiency and other parameters of TJSC. The calculated efficiency for TJSC is 37.2% for visible spectrum of light (400-700 nm) range. Fig. 9 shows the design structure along with tunnel junction, top coating, bottom contacts and anti-reflection coating of a TJSC and SJSC.

5. Results and Discussions

A TJSC (InGaN/ AlGaAs/ InGaAs) and a seven junction solar cell (InGaN/InGaN/AlInP/AlInP/AlGaAs/AlGaAs/ AlGaAs) is considered for the simulation of this model. Efficiencies calculated for UV, visible and IR light spectrum at different values of temperature and suns are presented in Table 2 & 3, respectively. Comparison of results of MJSC obtained from simulation techniques are presented in Table 5. The current voltage (I-V) and power voltage (P-V) curves plotted for TJSC in UV, Visible and IR spectrum respectively are shown in Fig. 10.

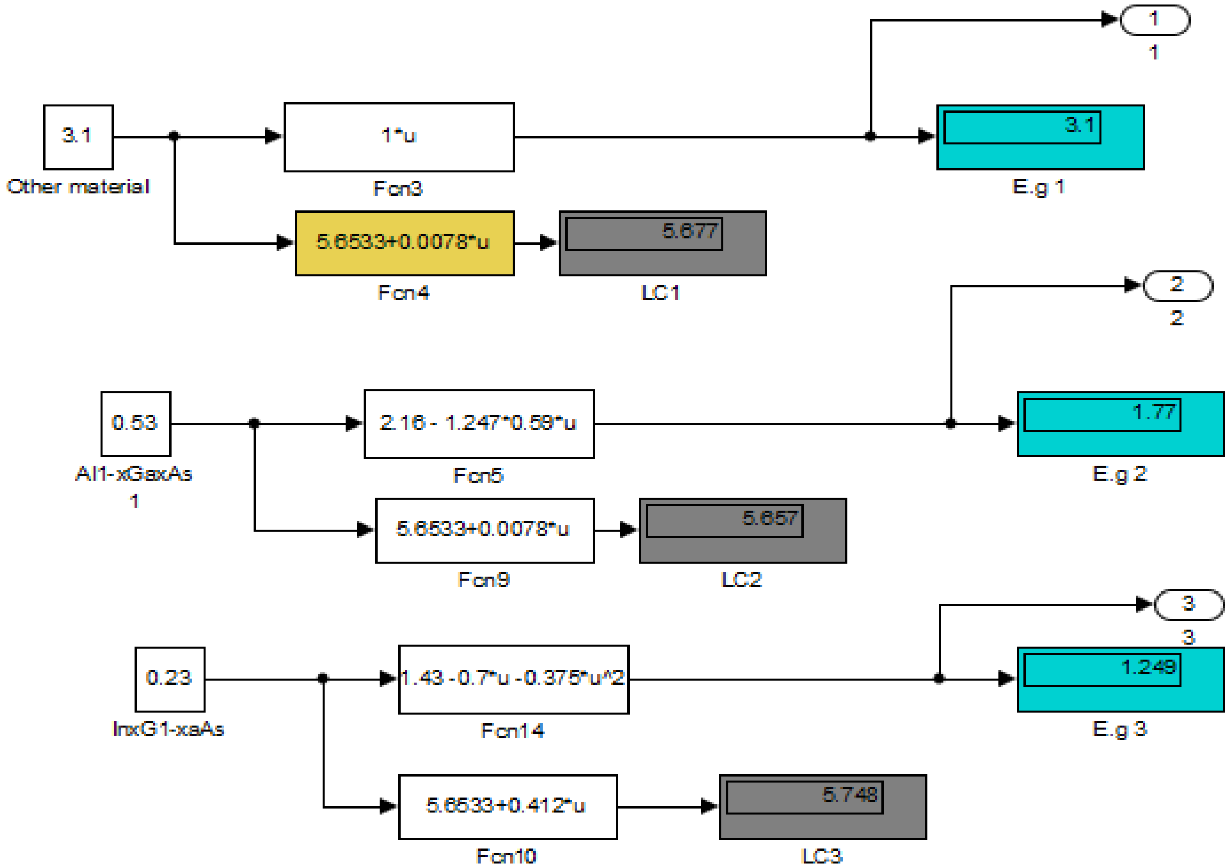

Fig. 7: E_g and LC for different composition of semiconductor materials.

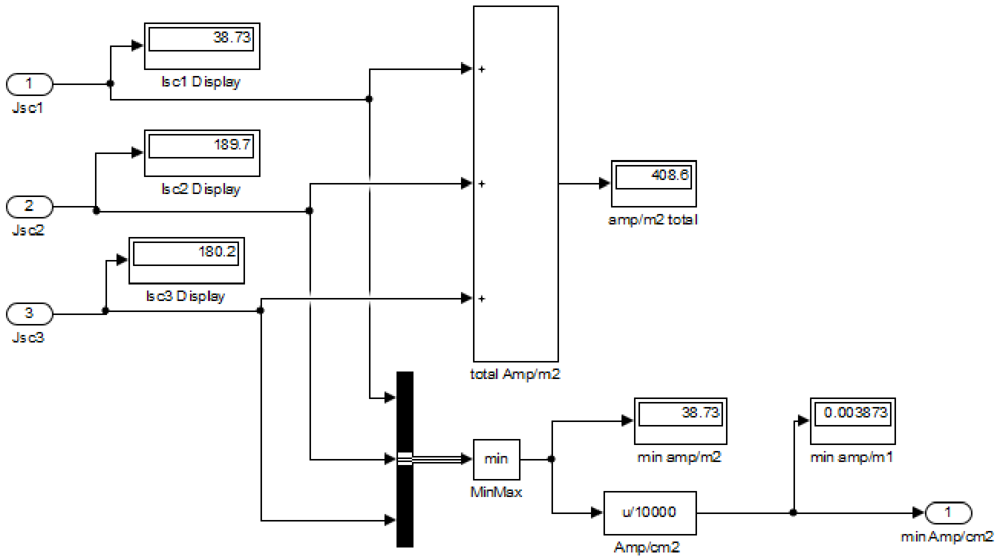

Fig. 8: J_{sc} (max) and J_{sc} (min).

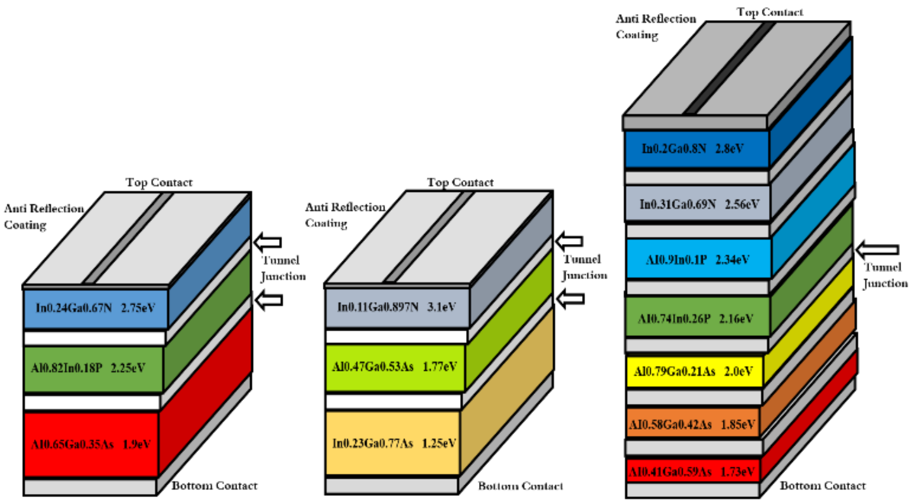

Fig. 9: MJSCs structures (a) Left: TJSC for visible light spectrum, (b) Centre: TJSC for UV, Visible and IR light spectrum, (c) Right: Seven junction solar cell for visible light spectrum.

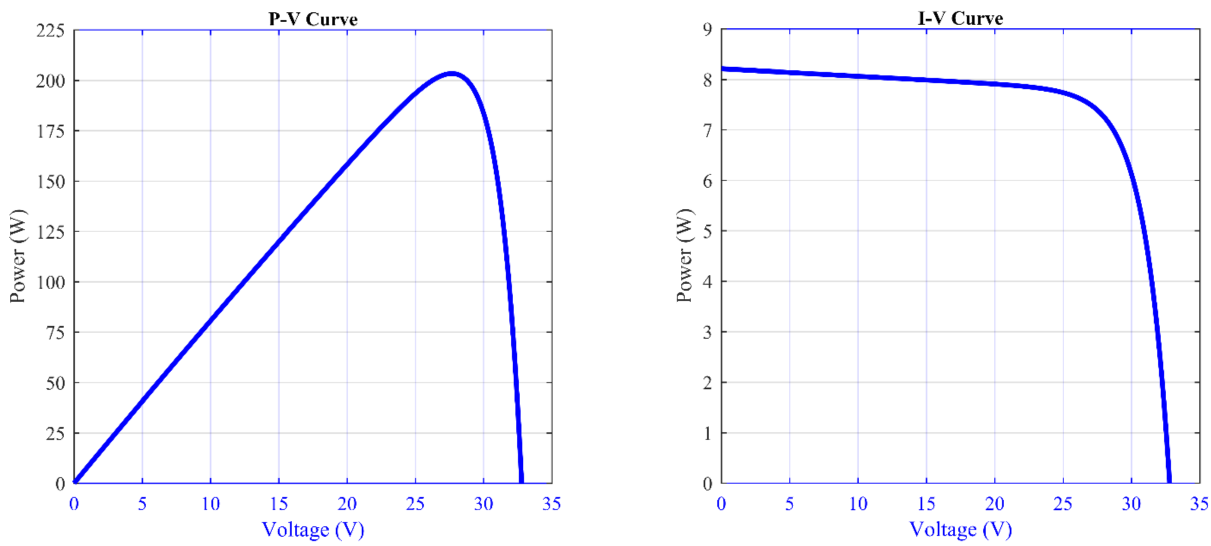

Fig. 10: P-V and I-V curves plotted for TJSC (UV, Visible and IR).

Table 2: Efficiency (%η) vs temperature (K) for 1 sun.

Temp (K)	200	225	250	275	300	325	350	375	400	600	1000
η(%) for Visible Spectrum	40.3	39.5	38.8	38	37.2	36.4	35.6	34.8	34.1	27.8	15.3
η(%) UV, Visible and IR Spectrum	23.98	23.47	22.98	22.46	21.95	21.45	20.98	20.43	19.93	15.88	9.23

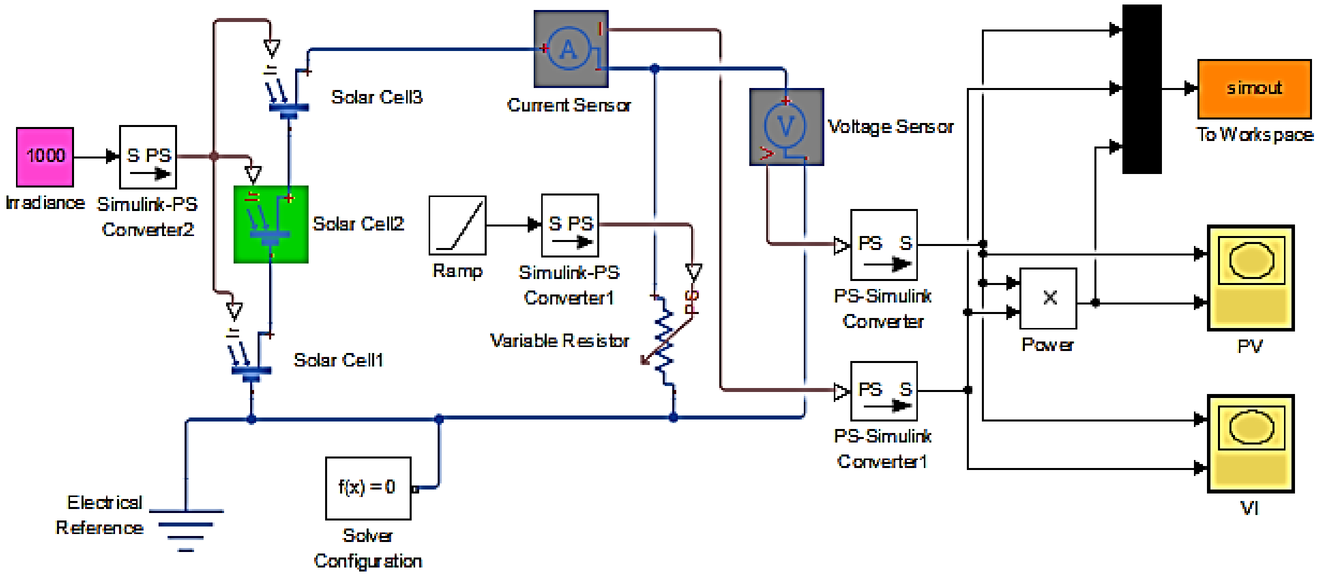

Fig. 11: Equivalent circuit of TJSC (Visible light spectrum).

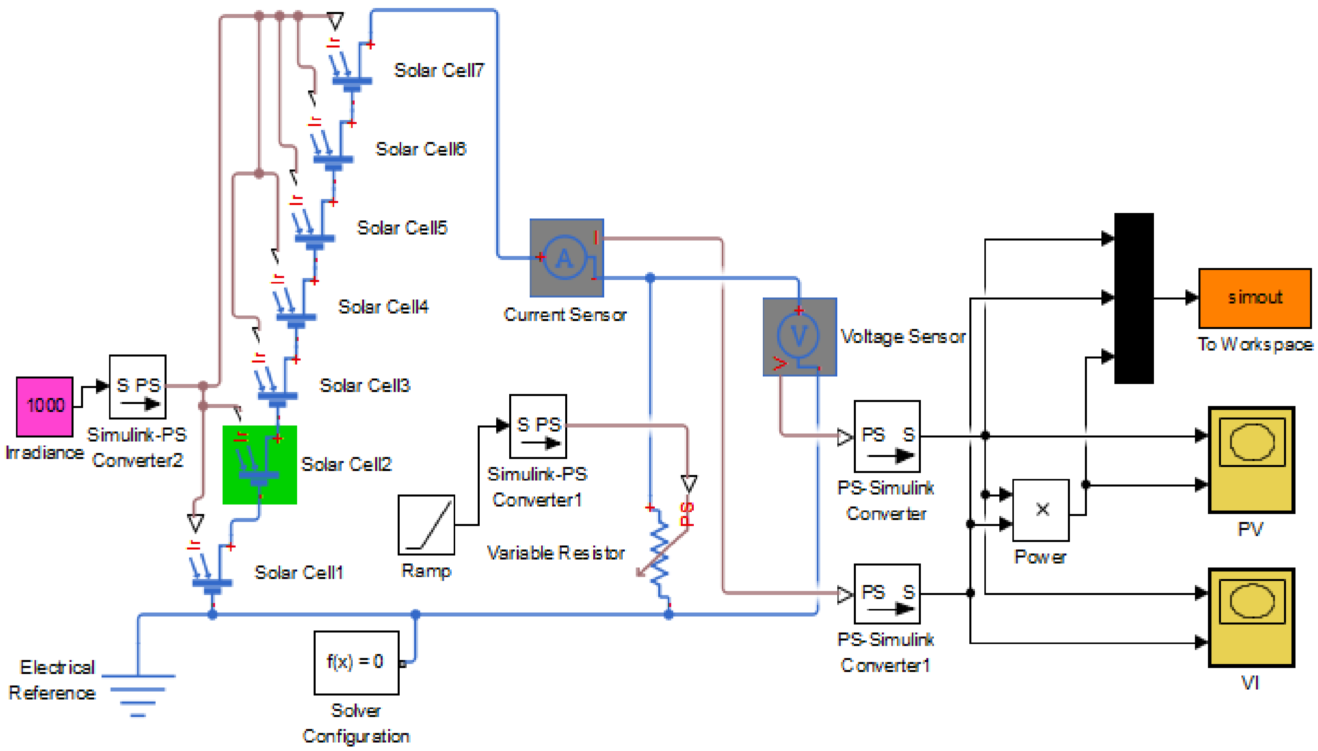

Fig. 12: Equivalent circuit of seven junction solar cell (Visible light spectrum).

Table 3: Efficiency (%η) vs suns for temperature 300K.

Sun	1	2	5	10	50	100	500	1000	2000	5000
η (%) for Visible spectrum	37.2	37.6	38	38.4	39.2	39.6	40.5	40.8	41.2	41.7
η (%) UV, Visible and IR spectrum	92	22.2	22.5	22.8	23.4	23.6	24.2	24.4	24.7	25

Table 4: MJSC parameters.

Materials	E_g (eV)	Wavelength (nm)	Power (P_{in}) (W/cm^2)	J_{sc} (mA/cm^2)	V_{oc} (V)
TJSC Visible Spectrum (400-650nm)					
$In_{0.24}Ga_{0.76}N$	2.8	400-450	0.0073	2.5	2.291
$Al_{0.82}In_{0.18}P$	2.3	450-550	0.0154	6.21	1.813
$Al_{0.65}Ga_{0.35}As$	1.9	550-650	0.0143	6.93	1.408
Total	-	400-650	0.0371	15.64	5.512
P_{in} = 371W/m^2P_{out} = 138.1W/m^2 η = 37.2 %					
TJSC UV, Visible and IR spectrum (100-1000nm)					
$In_{0.11}Ga_{0.89}N$	3.1	100-400	0.0145	3.873	2.653
$Al_{0.47}Ga_{0.53}As$	1.8	400-700	0.0431	18.97	1.362
$In_{0.23}Ga_{0.67}As$	1.3	700-1000	0.0268	18	0.78
Total	-	100-1000	0.0844	40.8	4.795
P_{in} = 844W/m^2P_{out} = 185.7 W/m^{2}η = 21.95%					
Seven Junction Solar Cell					
$In_{0.2}Ga_{0.8}N$	2.9	380-435	7.5	2.53	2.386
$In_{0.31}Ga_{0.69}N$	2.6	435-485	7.4	2.852	2.105
$Al_{0.9}In_{0.1}P$	2.3	485-530	7.2	2.888	1.822
$Al_{0.74}In_{0.26}P$	2.2	530-575	6.9	3.075	1.706
$Al_{0.79}Ga_{0.21}As$	2	575-620	6.8	3.168	1.551
$Al_{0.58}Ga_{0.42}As$	1.9	620-670	6.7	3.533	1.339
$Al_{0.41}Ga_{0.59}As$	1.7	670-720	6.5	3.482	1.214
Total	-	-	49	-	12.12

P_{in} = 49mW/cm^2
P_{out} = 30.66 mW/cm^2
η = 62.6%

Table 5: Comparison of MJSC parameters.

	TJSC for Visible spectrum	TJSC light spectrum of UV, Visible and IR spectrum	Seven Junction Solar Cell visible light spectrum
P_{out} (mW/cm^2)	13.18	18.57	30.66
P_{max} (mW/cm^2)	12.8	16.74	28.93
Fill Factor or F.F (%)	93	90	94.3
Efficiency (η)	37.2	21.9	62.6

5.1 MJSC P-V and I-V Characteristics Curves

The study of PV system requires precise knowledge about the nonlinear P-V and I-V output characteristics curves under different levels of irradiation [35, 36]. The characteristics curves of the solar cell provide knowledge about its functioning. The parameters (V_{oc}, J_{sc} and E_g) are provided in data sheet by the manufacturers or can be calculated from simulation [37, 38]. Load resistance can be varied from zero (short circuit) to infinity (open circuit). Values of voltage and current at different values of resistance can be calculated and plotted. P-V and I-V characteristics curves plotted for TJSC are shown in Fig. 10.

5.2 Equivalent Circuit for TJSC for Visible Light Spectrum

The equivalent circuit of TJSC and Seven Junction Solar Cell for visible light spectrum is shown in Fig. 11 and Fig. 12, respectively. The values of E_g, V_{oc} and J_{sc} obtained from simulation results can be placed in the solar cell block properties. Solar cell parameters are given in Table 4 [39]. Load resistance can be varied from lowest (short circuit) to the highest (open circuit) via a ramp signal. Values of current and voltage will be highest at maximum power point (P_{max}) [40].

5.3 Comparison of Results

From the simulations performed above, it is evident that the efficiency of TJSC is higher than the efficiency of seven junctions solar cell. Thermal loss and I^2R losses are also lower. Moreover, the efficiency of MJSC increases as the number of junctions increases. Efficiency for TJSC (InGaN/ AlGaAs/InGaAs) is comparatively low due to non-availability of suitable materials for UV, IR and visible light spectrum range [41]. Comparison of results of MJSC obtained from simulation techniques are presented in Table 5. It is recommended that other materials may be investigated so that the entire solar spectrum can be efficiently used.

6. Conclusions

In the simulation work performed, input power (P_{in}), bandgap energy (E_g), short circuit current (J_{sc}), leakage current (J_o), open circuit voltage (V_{oc}), output power (P_{out}) and % efficiency ($\%\eta$), have been calculated. The efficiency (η) of a MJSC can be increased by increasing number of junctions, current matching in each cell, equalizing short circuit current in each subcell, decreasing cell temperature and increasing irradiations. In MJSC, all the cells are connected in series. Due to flow of minimum current, efficiency decreases. However, efficiency can be increased by increasing voltage and light concentration. If MJSC efficiency (η) is low, all calculated parameters V_{oc}, J_{sc}, J_o and P_{in} are verified and adjusted accordingly. The generated current should be same for each cell. PV material should be selected to achieve the desired bandgap energy. Adjust the bandgap energy to match generated photocurrent and the LC of all cells. The bandgap energy for different PV materials can be achieved easily; however, LC matching is difficult. LC matching is essential in assembling MJSC. May be in future, advance research in new PV material compositions will make it possible.

References

[1] T. Katsuaki, “A review of ultrahigh efficiency iii-v semiconductor compound solar cells: multijunction tandem, lower dimensional, photonic up/down conversion and plasmonic nanometallic structures”, Energies, vol. 2, pp. 504-530, 2009.

[2] M. Ali, “Solar absorption air-conditioning systems”, ASHRAE/ PHVACR Expo and Conference Pakistan, 2011. [Online]. Available: https://www.semanticscholar.org/paper/Solar-Absorption-Air-Conditioning-Systems-Ali. [Accessed Nov. 11, 2018].

[3] F. Dimroth and S. Kurtz, “High-efficiency multijunction solar cells”, MRS bulletin, vol. 32, no. 3, pp. 230-235, 2007.

[4] B. Burnett, “The basic physics and design of III-V multijunction solar cells”, J. Electromagn. Anal. Appl., vol. 6, no. 13, November 2014.

[5] M.A. Green, “Photovoltaic principles”, Phys. E (Amsterdam, Neth.), vol. 14, no. 1, pp. 11-17, April 2002.

[6] M. Yamaguchi, T. Takamoto, K. Araki and N. Ekins-Daukes, “Multi-junction III–V solar cells: current status and future potential”, Sol. Energy, vol. 79, pp. 78-85, 2005.

[7] M. Yamaguchi, T. Takamoto, A. Khan, M. Imaizumi, S. Matsuda and N. Ekins-Daukes, “Super-high-efficiency multi-junction solar cells”, Prog. Photovoltaics, vol. 13, no. 2, pp. 125-132, 2005.

[8] A. Martí and A. Luque, “Next generation photovoltaics: High efficiency through full spectrum utilization”, CRC Press, 2003.

[9] R.R. King, N.H. Karam, J.H. Ermer, N. Haddad, P. Colter, T. Isshiki, H. Yoon, H.L. Cotal, D.E. Joslin, D.D. Krut and R. Sudharsanan, “Next-generation, high-efficiency III-V multijunction solar cells”, in Conference Record of the Twenty-Eighth IEEE Photovoltaic Specialists Conf.-2000, Anchorage, AK, USA, September 15-22, 2000, pp. 998-1001.

[10] M. González, N. Chan, N. Ekins-Daukes, J.G. Adams, P. Stavrinou, I. Vurgaftman, J.R. Meyer, J. Abell, R.J. Walters, C.D. Cress and P.P. Jenkins, “Modeling and analysis of multijunction solar cells”, Phys. and Simulation of Opt. Devices XIX, SPIE OPTO 2011, San Francisco, California, USA, February 21, 2011, International Society for Optics and Photonics, 2011, pp. 79330R.

[11] W. Guter, and A.W. Bett, "IV-characterization of devices consisting of solar cells and tunnel diodes", IEEE 4th World Conf. on PV Energy Conf., 7-12 May 2006, Waikoloa, HI, USA, vol. 1, pp. 749-752.

[12] R. Sven, "Tabulated values of the Shockley–Queisser limit for single junction solar cells", Sol. Energy, vol. 130, pp. 139-147, 2016.

[13] A. Blakers, N. Zin, K.R. McIntosh and F. Fong, “High efficiency silicon solar cells”, Energy Procedia, vol. 33, pp. 1-10, 2013.

[14] M.A. Green, K. Emery, Y. Hishikawa and W. Warta, "Solar cell efficiency tables (version 37)", Prog. Photovoltaics, vol. 19 pp. 84-92, 2010.

[15] M.J. Keevers, C.F.J. Lau, M.A. Green, I. Thomas, J.B. Lasich, R.K. Richard and A. Keith, “High efficiency spectrum splitting prototype sub-module using commercial CPV cells”, 6th World Conf. on Photovoltaic Energy Conversion, WCPEC-6, Kyoto, Japan, Nov. 23-27, 2014.

[16] G.K. Dey and T.A. Kazi, "Multi-junction solar cells and microwave power transmission technologies for solar power satellite", IEEE Int. Conf. on Inform., Electronics & Vision, ICIEV, Dhaka, Bangladesh (May 23-24, 2014), vol. 1, pp. 1-6, 2014.

[17] F. Dimroth, G. Matthias, P. Beutel, U. Fiedeler, C. Karcher, T. Tibbits, E. Oliva, G. Siefer, M. Schachtner, A. Wekkeli, A. Bett, R. Krause, M. Piccin, N. Blanc, C. Drazek, E. Guiot, B. Ghyselen, T. Salvetat, T. Signamarcheix, T. Hannappel, K. Schwarzburg, "Wafer bonded four-junction GaInP/ GaAs/ GaInAsP/ GaInAs concentrator solar cells with 44.7% efficiency", Prog. Photovoltaics, vol. 3, pp. 277-282, 2014.

[18] H. Cotal, C. Fetzer, J. Boisvert, G. Kinsey, R. King, P. Hebert, H. Yoon and N. Karam, "III–V multijunction solar cells for concentrating photovoltaics", Energy Environ. Sci., vol. 2, pp. 174-192, 2009.

[19] W. Guter, J. Schöne, S.P. Philipps, M. Steiner, G. Siefer, A. Wekkeli, E. Welser, E. Oliva, A. W. Bett and F. Dimroth, "Current-matched triple-junction solar cell reaching 41.1% conversion efficiency under concentrated sunlight", Appl. Phys. Lett. 94, vol. 22, pp. 1-12, 2009.

[20] M.A. Green, "Third generation photovoltaics: advanced solar energy conversion", Phys. Today, vol. 57, no. 12, pp. 71-72, 2004.

[21] R.R. King, "Raising the efficiency ceiling in multijunction solar cells", Energy Efficient Mater., vol. 1, pp. 1-76, 2011.

[22] M.A. Green, "Solar cell efficiency tables (version 54)", Prog. Photovoltaics, vol. 27, pp. 565-575, 2019.

[23] J.A. Gow and C.D. Manning, "Development of a photovoltaic array model for use in power-electronics simulation studies", IEEE Proc. of Electric Power Appl., vol. 146, no. 2, pp. 193-200, 1999.

[24] O. Wasynezuk, "Dynamic behavior of a class of photovoltaic power systems", IEEE Trans. Power Appar. Syst., vol. 9, pp. 3031-3037, 1983.

[25] J.C.H. Phang, D.S.H. Chan and J.R. Phillips, "Accurate analytical method for the extraction of solar cell model parameters", Electron. Lett., vol. 20, no. 10, pp. 406-408, 1984.

[26] H.L. Tsai, C. Tu and Y. Su, "Development of generalized photovoltaic model using Matlab/Simulink", Proc. of the WCECS, San Francisco, USA, (October 22 – 24), vol. 1, pp. 1-6, 2008.

[27] E.C. Warmann, M.S. Leite and H.A. Atwater, "Photovoltaic efficiencies in lattice-matched III-V multijunction solar cells with unconventional lattice parameters," 37th IEEE Photovoltaic Spec. Conf., Seattle, WA, USA (June 19-24), vol. 1, pp. 1-5, 2011.

[28] P. Singh, and N. Ravindra, "Temperature dependence of solar cell performance - an analysis", Sol. Energy Mater. Sol. Cells, vol. 101, pp. 36-45, 2011.

[29] I. Vurgaftman, J. Meyer and L. Ram-Mohan, "Band parameters for III–V compound semiconductors and their alloys", J. Appl. Phys., vol. 89, no. 11 pp. 5815-5875, 2001.

[30] A. Shukla, M. Khare and K.N. Shukla, "Modeling and simulation of solar PV module on Matlab/Simulink", Int. J. Innovative Res. Sci., Eng., Technol., vol. 4, no. 1, pp. 18516- 18527, 2015.

[31] P. Bhattacharya, R. Fornari and H. Kamimura, "Comprehensive Semiconductor Science and Technology", vol. 1, Elsevier Newnes; 2011.

[32] M.A. Ali, G. Subhani and S. Akram, "Economic viability of solar absorption cooling system in Pakistan", Int. J. Adv. Study Res. Work, vol. 1, pp. 7-14, 2018.

[33] E. F. Fernández, A. J. García-Loureiro and G. P. Smestad, "Multijunction concentrator solar cells: analysis and fundamentals", in High Concentrator Photovoltaics, pp. 9-37. Springer, Cham, 2015, pp. 9-37.

[34] S. Lansel, "Technology and future of III-V multi-junction solar cell", Int. J. Appl. Phys., vol. 6, no. 3, pp. 3-8, 2010.

[35] E. Olías, A. Barrado and A. Lázaro, "Review of the maximum power point tracking algorithms for stand-alone photovoltaic systems", Sol. Energy Mater. Sol. Cells, vol. 90, no. 11, pp. 1555-1578, 2006.

[36] B. Subudhi and R. Pradhan, "A Comparative Study on Maximum Power Point Tracking Techniques for Photovoltaic Power Systems", IEEE Trans. on Sustainable Energy, vol. 4, no. 1, pp. 89-98, 2013.

[37] L. Castaner and S. Silvestre, Modelling photovoltaic systems using PSpice, John Wiley and Sons, 2002.

[38] B.S. Richards and K.R. McIntosh, "Overcoming the poor short wavelength spectral response of CdS/CdTe photovoltaic modules via luminescence down-shifting: ray-tracing simulations", Prog. Photovoltaics, vol. 15, no. 1, pp. 27-34, 2007.

[39] T. Easwarakhanthan, J. Bottin, I. Bouhouch and C. Boutrit, "Nonlinear minimization algorithm for determining the solar cell parameters with microcomputers", Int. J. Sol. Energy, vol. 4, no. 1, pp. 1-12, 2015.

[40] K. A. Emery and C. R. Osterwald, "Solar cell efficiency measurements", Sol. Cells, vol. 17, no. 2, pp. 253-274, 1986.

[41] C. Maurya, A. K. Gupta, P. Srivastava, L. Bahadur, "Callindra haematocephata and Peltophorum pterocarpum flowers as natural sensitizers for TiO_2 thin film based dye-sensitized solar cells", Opt. Mater., vol. 60, pp. 270-6, 2016.